HOW MANY *M* FORMS ARE THERE IN THE BACTERIORHODOPSIN PHOTOCYCLE?

G. I. GROMA AND Zs. DANCSHÁZY
Institute of Biophysics, Biological Research Center of Hungarian Academy of Sciences, P.O.B. 521, 6701 Szeged, Hungary

ABSTRACT On capturing a quantum of light, the bacteriorhodopsin of *Halobacterium halobium* undergoes a photocycle involving different intermediates. The exact scheme of the photocycle and especially the number of *M* intermediates are subjects of debate. For a quantitative analysis of many effects connected with the photocycle, e.g. the effect of the membrane potential on the kinetics of *M* decay (Groma et al., 1984. *Biophys. J.* 45:985–992), a knowledge of the exact photocycle is needed. In the present work sophisticated measurements were made on the decay kinetics of the *M* forms in cell envelope vesicles, purple membrane suspension and purple membrane fragments incorporated in polyacrylamide gel. The experimental data were analyzed by fitting one, two, and three discrete exponentials. Three different real components were found in the *M* decay of cell envelope vesicles in 4 M NaCl. All of them exhibited a temperature-dependence obeying the Arrhenius law. Two real components were found for the purple membrane in suspension and in gel in NaCl-free medium. The third phase appeared when the gel was soaked in 4 M NaCl. As an independent means of analysis, a continuous distribution of exponentials was also fitted to the *M* decay kinetics in cell envelope vesicles. This calculation also resulted in three processes with distinct rates or alternatively two processes with distributed rates.

INTRODUCTION

Bacteriorhodopsin (bR), the single protein of the purple membrane of *Halobacterium halobium,* utilizes the energy of light to build up a proton electrochemical potential across the cell membrane. The proton pump is accompanied by a photocycle of several intermediates, distinguished by the absorption properties of the retinal chromophore. Although the scheme of the photocycle has been the subject of numerous studies, several contradictions remain in this field. The majority of these relate to the mechanism of decay of the long-lived *M* intermediate.

The original model of the bR photocycle was a sequence of unidirectional unbranching first-order reactions (1). It contained only one *M* form. Later an increasing number of observations indicated biphasic *M* decay. Several authors found two *M* forms even at low ionic strength and neutral pH (2–9), whereas others did so only at high ionic strength (10-14) or at high pH (15–18). Recently, differences were observed in the proton pumping functions (14) and the absorption spectra (19) of two kinetically different forms, while their resonance Raman spectra were found to be identical (20). Unfortunately, a quantitative computer analysis of the experimental data has been carried out in only some of these studies (5–7, 9, 11, 16, 19). At the same time, if graphical methods are used to evaluate the kinetic curves, the exact number of components remains highly uncertain. Nagle and coworkers recently started a systematic computer analysis to determine the detailed scheme of the bR photocycle (9, 21). They found that it certainly cannot be described by unidirectional unbranching sequence of first-order reactions.

In our previous studies we investigated the kinetics of *M* decay under physiological conditions, i.e. in intact cells (22, 23) and in cell envelope vesicles (24) in the presence of a membrane potential. The kinetics was never found to be monophasic. With two exponentials, satisfactory fits were achieved (24). Anomalies were observed, however, in the membrane potential-dependence of the kinetic parameters. The formulas used to determine these dependences are rather sensitive to the model used. One reason for the anomalies could be that even more components should be taken into account in the kinetics of *M* decay.

The aim of this work was to reduce the above discrepancies by using a sophisticated computer fitting of different numbers of exponentials to determine the exact decay kinetics of the *M* intermediate. We found that in cell envelope vesicles and also in purple membrane fragments at high ionic strength a third component is involved in the kinetics.

The experimental data were also analyzed by continuous distribution of exponentials, assuming less than three main *M* forms, but numerous slightly different conformational substates.

MATERIALS AND METHODS

Preparation of Samples

The preparation of *Halobacterium halobium* cell envelope vesicles has been described elsewhere (24). Vesicles were resuspended with 4 M NaCl

in 50 mM HEPES buffer (Sigma Chemical Co., St. Louis, MO, pH 7.0). For control measurements, purple membrane was prepared by standard methods (25). One fraction of purple membrane fragments was suspended in 10 mM HEPES buffer, pH 7.0. Since purple membranes tend to aggregate in 4 M NaCl, another fraction was immobilized in polyacrylamide gel (26). This sample was divided into two parts. One was soaked in 1 mM HEPES buffer, pH 7.0, the other in 4 M NaCl + 30 mM HEPES, pH 7.0. The samples were exposed to these media at least overnight.

Flash Photometric Measurements

Flash photometric measurements were carried out in a home-made set-up. A monitoring beam from a 250 W tungsten lamp (Tungsram 50550, Hungary) was passed through a 425-nm interference filter (10-nm halfwidth, Karl Zeiss Jena, German Democratic Republic) and split into two fractions. The main fraction was focused onto a 1-mm optical pathlength cell containing the sample, and was detected by a semiconductor photodiode (mode P1110, Alphametrics Ltd., Winnipeg, Canada). This detector was housed together with a home-made preamplifier (0.1-ms rise time). The reference beam was focused directly onto another photodiode (PIN-5 UV, United Detector Technology, Hawthorne, CA) combined with a preamplifier. Both detectors were protected from the actinic flash by band pass glass filters. The signals from the two preamplifiers were fed into a differential amplifier (model 604; Keithley Instruments, Inc., Cleveland, OH) with a high cut filter at 1 kHz. By this method the instability of the monitoring beam was reduced significantly. The amplified signal was digitized and stored in a transient recorder (8-bit resolution, 1024 channels, KFKI NEO 200, Hungary). 100–200 signals were averaged by a CAMAC data acquisition system (KFKI, Hungary) (27). The unit gain output of the individual channels of the differential amplifier was read on a digital voltmeter and was used to calculate the absolute OD changes. (No correction was made for light scattering.)

The actinic light from a high pressure xenon flash lamp (ShS−100, USSR, pulse width = 2 μs) was passed through heat filters (S3S−16, −24, −25, and −26) and low cut filters (ZhS−17 and −18, Mashinostroienie, USSR). This filter combination defined a spectral range of 520–630 nm. The actinic light was focused onto the sample at ~45°.

Recently it was found that in vesicular systems high intensity actinic flashes can build up significant membrane potential, which alters the kinetics of *M* decay (22). This potential can be eliminated by adding ionophores or by keeping the intensity and repetition rate of flashes at low level. To avoid some direct effect of the ionophores on the decay kinetics we choose the latter method. Using ~5 J/m^2 flash intensity and 0.5 Hz repetition rate, further reduction of these parameters caused no changes in the kinetics.

The concentrations of all samples were adjusted to approx. 0.3 OD in the 1-mm cell. The cell holder was thermostated and the exact temperature of the sample (within 0.1°C) was measured by a thermocouple immersed in it. The signal-to-noise ratio in the absorption kinetic measurements (after averaging) was ~300.

Fitting of Experimental Data with Discrete Exponentials

The fitting of discrete exponentials to the experimental curves was carried out with the SPSERV program of Bagyinka (28) using a least-square method. In this program the number of exponentials and the initial guesses for the fitting parameters are determined by the user. The baseline was calculated from the pretrigger part of the traces. Only the decaying parts of the absorption kinetic signals were fitted. In the output the program gives the time constants and amplitudes fitted, their errors and the standard deviation. These errors depend on the goodness of fit and the statistical noise in the experimental curves and will be referred to as error-1 in the text. Parameters from two independent measurements were averaged; the error of this averaging will be referred to as error-2.

Fitting with Continuous Distribution of Exponentials

Evaluation of the experimental curves by a continuous distribution of exponentials means solving the integral equation

$$y(t) = \int_0^\infty \exp(-kt)\, g(k)\, dk, \qquad (1)$$

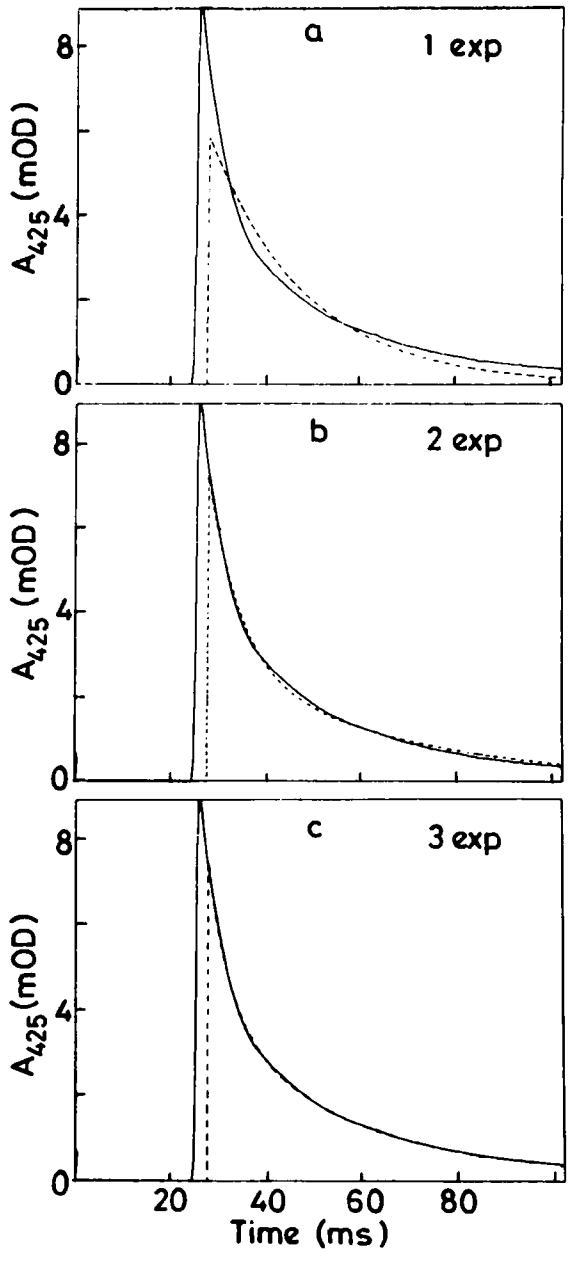

FIGURE 1 Fitting of the absorption kinetic signal of the decay of the *M* form of bacteriorhodopsin in cell envelope vesicles in 4 M NaCl/50 mM HEPES buffer, pH 7.0. with different numbers of exponentials. Continuous line: measured absorbance changes at 425 nm at 20°C with dwell time = 0.4 ms (the first quarter of the total signal is shown). Dashed line: the fitting curve with (*a*) one, (*b*) two, and (*c*) three exponentials. To avoid the effect of rising part of the signal, the range where the fitting was performed was started from the 9th point following the pretrigger range. See Table I for the fitting parameters.

where $y(t)$ represents the experimental curve and $g(k)$ is the distribution function of rate constants to be determined. The solution of Eq. 1, however, is an ill-posed problem: arbitrarily small error in $y(t)$ can lead to an arbitrarily large error in $g(k)$. For this reason in general not the exact solution of Eq. 1 is looked for, but $g(k)$ is determined by fitting methods. We used the CONTIN program of Provencher to calculate $g(k)$. The detailed calculation procedure is described in references 29 and 30. The main advantage of this program is that it does not require any a priori knowledge of the analytical form of $g(k)$. To further reduce the ill-posed nature of the problem, CONTIN looks for a regularized (smooth) solution. Instead of minimizing the variance

$$\text{var} = \sum_{i=1}^{N_y} \left[y_i - \sum_{k=1}^{N_g} g_k \exp(-ik) \right]^2 \qquad (2)$$

it looks for a solution satisfying

$$\text{var} + \alpha^2 \sum_{k=1}^{N_y-2} (s_k)^2 = \text{minimum}, \qquad (3)$$

where the set of y_i and g_k represent the discrete points in $y(t)$ and $g(k)$, respectively, N_y and N_g are the numbers of points in the two sets, α is the regularization parameter and s_k are the second differences of the y_i set, corresponding to the second derivative of $y(t)$. In our case $N_y = 200$ (by compressing the dataset and cutting off the end tail) and $N_g = 40$. $g_k > 0$ was an additional regularizing condition. Different values of α provide a set of differently smoothed solutions and the user has to select the right one via additional criteria.

RESULTS AND DISCUSSION

Fig. 1 shows the absorption kinetic signal corresponding to the decay of the *M* forms in *H. halobium* cell envelope vesicles and the fitting curves using one, two, and three exponentials. Clearly, the one-exponential fit is rather poor. Visually, two exponentials give a satisfactory fit and with three there is no difference between the experimental and the fitting curve. The magnified residuals in Fig. 2 provide more information about the goodness of fitting. The residuals in Fig. 2 *a* (one exponential) are rather large and structured, reflecting the bad fit. Fig. 2 *b* (two exponentials) also shows a definitive structure in the residuals. It contains a long tail, which is completely missing in Fig. 2 *c* (three exponentials). The remaining short structured part in the beginning of Fig. 2 *c* is negligible (~1% of the original signal). Generally, the SPSERV program was not able to fit a fourth exponential to the experimental curves.

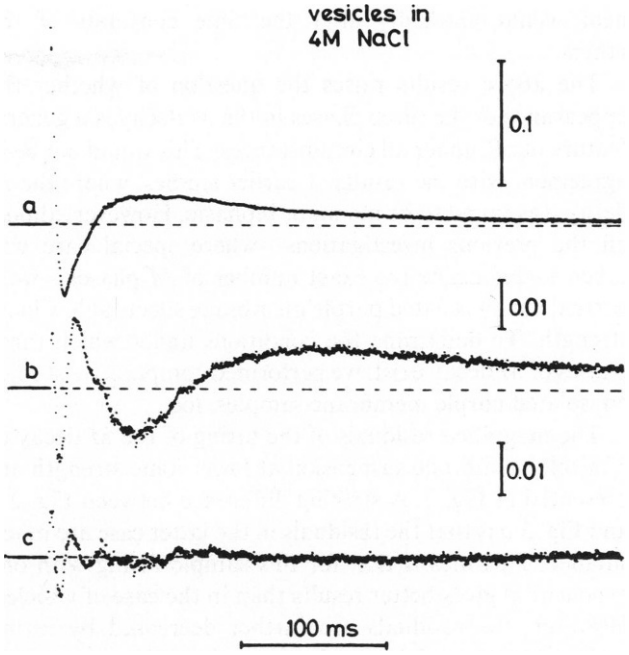

FIGURE 2 Magnified residuals (experimental curve – fitting curve) corresponding to the fitting of the *M* decay kinetics in cell envelope vesicles (see Fig. 1). Fitting with (*a*) one; (*b*) two; and (*c*) three exponentials. The residuals were normalized to the maximum of the experimental curve and the numbers on the vertical scale represent fractions of this maximum. See Table I for the fitting parameters.

The fitting parameters, their errors and the standard deviations for cell envelope vesicles are presented in Table I. Increasing the number of exponentials causes an approximately threefold decrease in the standard deviations. Though the relative weight of the third component is small, both error-1 and error-2 (see Materials and Methods for the meaning of these parameters) are also relatively small. Thus, Fig. 2 and Table I suggest that the third exponential in the *M* decay in cell envelope vesicles is a valid one and is not some fitting artefact. Note that neglect of this compo-

TABLE I
KINETIC PARAMETERS (A_i = AMPLITUDES AND τ_i = TIME CONSTANTS) FITTED TO THE DECAY OF THE *M* FORMS IN CELL ENVELOPE VESICLES IN 4 M NaCl

	One-exponential fit			Two-exponential fit			Three-exponential fit		
	Value	Error-1	Error-2	Value	Error-1	Error-2	Value	Error-1	Error-2
A_1*	1.000	0.009	0.009	0.702	0.008	0.004	0.630	0.004	0.002
τ_1‡	20.5	0.2	0.01	6.2	0.1	0.3	4.3	0.04	0.2
A_2	—	—	—	0.30	0.005	0.01	0.35	0.002	0.01
τ_2	—	—	—	37	0.4	1	26	0.1	1
A_3	—	—	—	—	—	—	0.018	0.0005	0.005
τ_3	—	—	—	—	—	—	240	8	50
S§	18.4	—	0.2	6.6	—	0.3	1.8	—	0.2

*The sum of the amplitudes is normalized to 1.
‡In milliseconds.
§S = (standard deviation)/(maximum of signal) × 10^3.

nent would markedly alter the time constants of the others.

The above results raises the question of whether the appearance of the three phases in the *M* decay is a general feature of bR under all circumstances. This would not be in agreement with the results of earlier studies, where the *M* decay was found to be mono- or biphasic. However, almost all the previous investigations—where special care was taken to determine the exact number of *M* phases—were carried out on isolated purple membrane sheets at low ionic strength. To determine the conditions under which three phases of *M* decay exist, we performed comparative studies on isolated purple membrane samples, too.

The magnified residuals of the fitting of the *M* decay in a purple membrane suspension at lower ionic strength are presented in Fig. 3. A striking difference between Fig. 2 *a* and Fig. 3 *a* is that the residuals in the latter case are much smaller. This means that for this sample fitting with one exponential gives better results than in the case of vesicles. However, the residuals are further decreased by fitting with two exponentials. At the same time, there is no long tail in Fig. 3 *b*, and this curve is practically identical with that in Fig. 3 *c*. Table II contains the fitting parameters for this sample. Here the standard deviation for one-exponential fitting is close to that for two-exponential fitting, shown in Table I. There is a twofold decrease in the standard deviation when two exponentials are used, but the third component practically does not reduce it further. The weight of the third component is extremely small (0.13%), and its time constant is extremely large: 500 ms (the whole time range of the measurement was 200 ms). Both error parameters are large and error-1 > error-2 indicating a high uncertainty even of the individual fittings. If the third exponential is neglected, the time constants of the others are practically unchanged. Accordingly, it is quite clear that this component is rather an artefact of fitting. Hence, our result is basically in agreement with those of other authors (2–9), who found two exponentials in the *M* decay in a purple membrane suspension at low ionic strength and neutral pH. However, we never observed a good fit using a single exponential under any conditions. Ohno and coworkers (17) observed that at high flash intensity the kinetics of *M* decay becomes biphasic and the amplitude of the slow component has a nonlinear function on light intensity. It was shown that this second transition appears when more molecules are excited in a bR trimer. Since the intensity of our flashes was far less than the range where this saturation effect was observed, the existence of two components in our data can not be interpreted in this way.

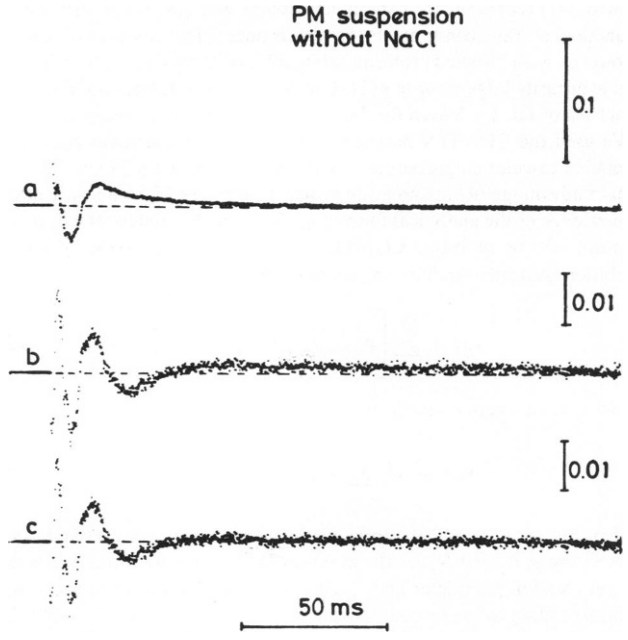

FIGURE 3 Magnified residuals corresponding to the fitting of the *M* decay kinetics in a purple membrane suspension in 10 mM HEPES buffer, pH 7.0, measured with dwell time = 0.2 ms at 20°C. Fitting with (*a*) one; (*b*) two; and (*c*) three exponentials. For other parameters see legends of Figs. 1 and 2 and Table II.

Fig. 4 and Table III present the results of fitting in the case of purple membrane incorporated in polyacrylamide gel. They show a picture qualitatively identical to that for the purple membrane in suspension. Here, the weight of the third component is a little higher, but still negligible.

Incubation of the gel containing purple membrane in 4 M NaCl markedly changes the kinetics of *M* decay. As

TABLE II
KINETIC PARAMETERS FITTED TO THE DECAY OF THE *M* FORMS IN PURPLE MEMBRANE SUSPENSION WITHOUT NaCl

	One-exponential fit			Two-exponential fit			Three-exponential fit		
	Value	Error-1	Error-2	Value	Error-1	Error-2	Value	Error-1	Error-2
A_1*	1.000	0.003	0.005	0.61	0.02	0.004	0.56	0.02	0.005
τ_1	6.58	0.02	0.01	3.96	0.08	0.01	3.77	0.10	0.02
A_2	—	—	—	0.39	0.02	0.0006	0.44	0.02	0.009
τ_2	—	—	—	9.7	0.2	0.02	9.1	0.2	0.1
A_3	—	—	—	—	—	—	0.0013	0.0003	0.0002
τ_3	—	—	—	—	—	—	500	700	200
S	6.412	—	0.005	2.98	—	0.05	2.78	—	0.002

*Notations as in Table I.

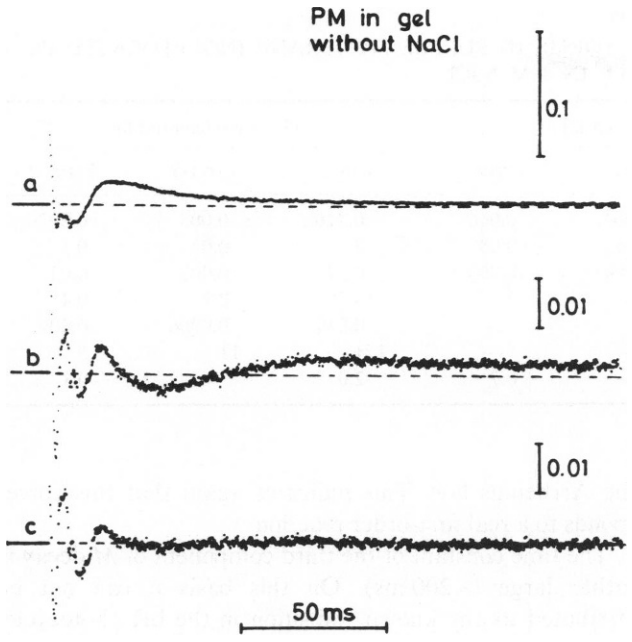

FIGURE 4 Magnified residuals corresponding to the fitting of the *M* decay kinetics in purple membrane incorporated in polyacrylamide gel in 1 mM HEPES buffer, pH 7.0, measured with dwell time = 0.2 ms at 20°C. Fitting with (*a*) one; (*b*) two; and (*c*) three exponentials. For other parameters see legends of Figs. 1 and 2 and Table III.

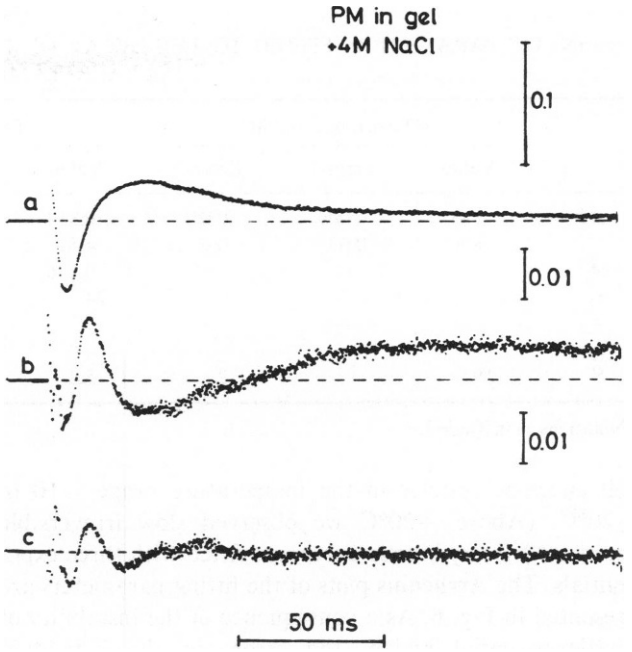

FIGURE 5 Magnified residuals corresponding to the fitting of the *M* decay kinetics in purple membrane incorporated in polyacrylamide gel in 4 M NaCl/1 mM HEPES buffer, pH 7.0, measured with dwell time = 0.2 ms at 20°C. Fitting with (*a*) one; (*b*) two; and (*c*) three exponentials. For other parameters see legends of Figs. 1 and 2 and Table IV.

Fig. 5 *a* shows, the residuals of the single-exponential fit are highly increased. The long tail again exists in the residuals of the two-exponential fit (Fig. 5 *b*), but disappears when three exponentials are fitted (Fig. 5 *c*. The fitting parameters listed in Table IV show an increase in the weight of the third component and a realistic value and errors for the time constant. The standard deviation of the single-exponential fit is increased compared to the NaCl-free sample. However, the standard deviation decrease more and more when two and three exponentials are fitted. All of these features highly resemble those for cell envelope vesicles.

The above results can be summarized as follows. At low ionic strength, purple membranes in suspension or in polyacrylamide gel show a biphasic decay of the *M* intermediate. In 4 M NaCl, however, a third component appears in both purple membrane fragments and cell envelope vesicles. In the vesicles the time constants are slightly higher than in the gel, but otherwise the two systems behave similarly. The weight of the third component is low (2%) but its existence is obvious from the results of fitting. This tendency is qualitatively in agreement with the observations of other authors (10, 13) who found a monophasic *M* decay at low ionic strength, but a biphasic one at high ionic strength. The larger number of components in our case is probably due to the better quality of the measurements (higher signal-to-noise ratio) and the application of sophisticated computer fitting instead of graphical analysis.

To find further proof of the validity of the third process mentioned above, we measured the kinetics of *M* decay in

TABLE III
KINETIC PARAMETERS FITTED TO THE DECAY OF THE *M* FORMS IN PURPLE MEMBRANE INCORPORATED IN POLYACRYLAMIDE GEL WITHOUT NaCl

	One-exponential fit			Two-exponential fit			Three-exponential fit		
	Value	Error-1	Error-2	Value	Error-1	Error-2	Value	Error-1	Error-2
A_1*	1.000	0.004	0.0006	0.88	0.005	0.01	0.767	0.009	0.0008
τ_1	6.66	0.03	0.06	5.0	0.04	0.2	4.45	0.05	0.09
A_2	—	—	—	0.12	0.005	0.02	0.23	0.01	0.004
τ_2	—	—	—	19	0.4	2	12.0	0.3	0.005
A_3	—	—	—	—	—	—	0.005	0.0004	0.001
τ_3	—	—	—	—	—	—	800	600	600
S	8.57	—	0.06	3.3	—	0.1	2.0	—	0.1

*Notations as in Table I.

TABLE IV

KINETIC PARAMETERS FITTED TO THE DECAY OF THE *M* FORMS IN PURPLE MEMBRANE INCORPORATED IN POLYACRYLAMIDE GEL IN 4 M NaCl

	One-exponential fit			Two-exponential fit			Three-exponential fit		
	Value	Error-1	Error-2	Value	Error-1	Error-2	Value	Error-1	Error-2
A_1*	1.00	0.009	0.02	0.814	0.004	0.006	0.716	0.003	0.007
τ_1	8.8	0.09	0.6	4.51	0.05	0.08	3.7	0.03	0.1
A_2	—	—	—	0.186	0.004	0.003	0.27	0.003	0.02
τ_2	—	—	—	24	0.3	2	15.7	0.2	0.4
A_3	—	—	—	—	—	—	0.019	0.0006	0.002
τ_3	—	—	—	—	—	—	171	11	5
S	19	—	2	5.3	—	0.7	2.0	—	0.1

*Notations as in Table I.

cell envelope vesicles in the temperature range −10 to +20°C. (Above +20°C we observed slow irreversible processes.) Every kinetic curve was fitted with three exponentials. The Arrhenius plots of the fitting parameters are presented in Fig. 6. As a consequence of the instability of multiexponential fitting, the errors in the individual parameters are high and do not allow calculation of the activation enthalpies and frequency factors. Clearly, the three processes differ more in their frequency factors than in their enthalpies. The relative amplitudes are practically temperature-independent. From our viewpoint, the important information from this figure is that the third process displays a temperature-dependence which basically obeys the Arrhenius law. This indicates again that this corresponds to a real first-order reaction.

The time constant of the third component of *M* decay is rather large (~200 ms). On this basis it can not be attributed to any known transition in the bR photocycle. Recently, Der and coworkers (26) also observed a long-lived (80 ms) component at 403 nm in 100 mM KCl. Our preliminary measurements on the wavelength-dependence of the amplitude of this process indicate a maximum at around 400 nm. This means that it corresponds to the decay of an *M*-like intermediate and is not due to the tail of the absorption of another intermediate or to a light scattering change.

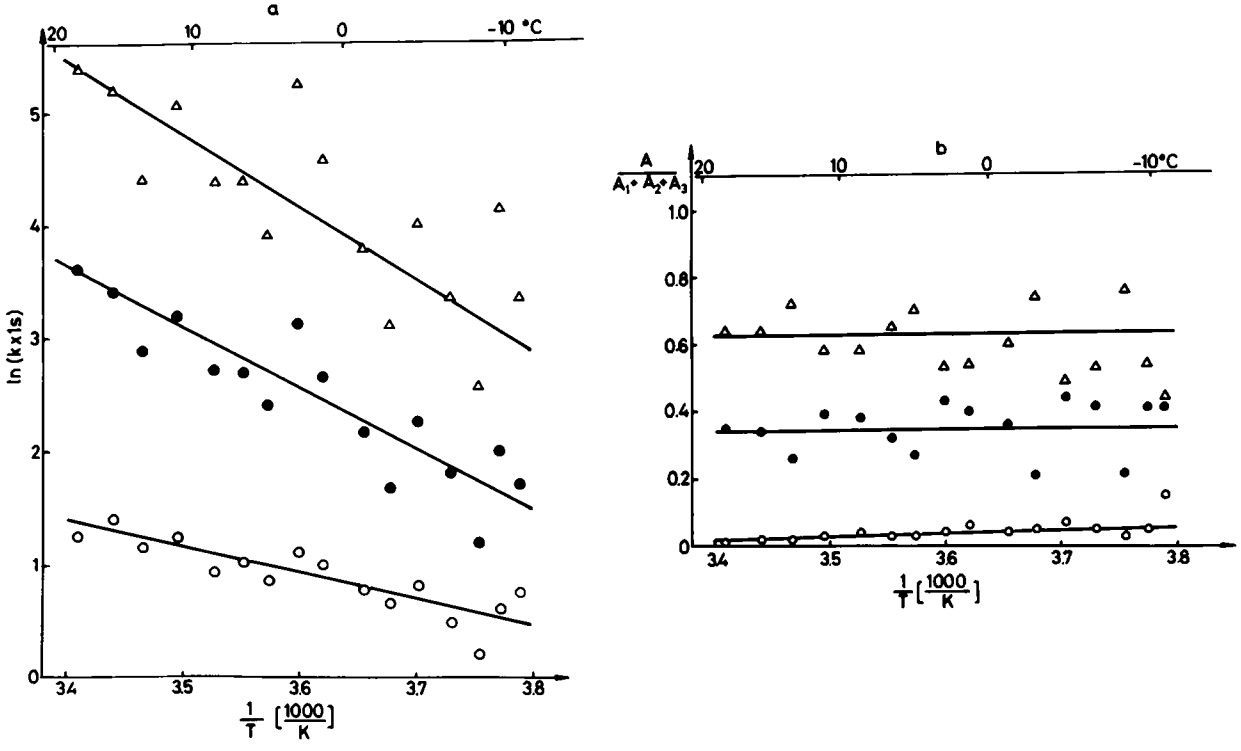

FIGURE 6 Temperature-dependence of the fitting parameters of the *M* decay in cell envelope vesicles in 4 M NaCl/50 mM HEPES buffer, pH 7.0. Kinetic curves at all temperatures were fitted with three exponentials. (*a*) Arrhenius plot of rate constants determined by the fitting. (*b*) Relative amplitudes of the individual processes. △, fastest; ●, intermediate; and ○, slowest process.

Numerous different models can be created to describe an M decay of three components. Some of these can be excluded, however, on the basis of the constraint relations among the time constants and amplitudes. We recently showed that, if two different M intermediates exist in the photocycle, they can not be formed sequentially, but a branching should take place in the photocycle (24). A model in which branching appears before the M states and two M forms decay in parallel was consistent with the experimental data. If the same type of analysis is used for three components, one can easily conclude the following:

(*a*) If three different M forms occur in parallel all the amplitudes must be positive.

(*b*) If at least two of three M intermediates are in sequence, at least one amplitude should be negative.

(*c*) One can get an apparent M decay of three components with less than three different M forms allowing back-reaction(s) from O intermediate(s). In this case at least one amplitude should be negative.

Since all the amplitudes were found to be positive, we suggest the existence of three parallel M intermediates. These can originate from branching(s) in the earlier part of the photocycle. Alternatively, a mixture of three different bR forms can exist even in the ground state. Hanamoto and coworkers (31) suggested that different protonation states of a tyrosine residue near the chromophore could cause the appearance of the two M forms measured. Other residues (even if they are far from the chromophore) could have a similar effect. The importance of the cation binding of the purple membrane was recently recognized (19, 32, 33). When deionized membranes were reconstituted with different cations, different kinetics of the photocycle were measured (19, 33). Hence, the existence of different states of cation binding could also explain the multiphasic nature of the M decay. The dependence of the number of phases on the ionic strength is consistent with this explanation.

It is clear that describing the nature of the different forms in physical term requires many additional studies of different methods. However, we would like to point out that simply the existence of them has important consequences on the understanding of bR photocycle. To illustrate this we suppose three parallel M forms in the following simplified photocycle:

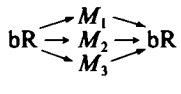

Scheme I

The bR $\rightarrow M_i$ transition is supposed to be instanteous after excitation. The differential equation system describing the M decays in the presence of constant illumination is

$$\dot{[M_i]} = -[M_i]/\tau_i + \sigma\phi f_i(1 - [M_1] - [M_2] - [M_3])$$
$$i = 1, 2, 3, \qquad (4)$$

where f_i is the probability that bR goes to M_i, τ_i is the lifetime of M_i, ϕ is the intensity of the illumination, σ is the product of the absorption cross section of bR and the quantum yield of photocycle, and the total amount of bR is normalized to 1.

The solution of Eq. 4 will be studied under three different conditions frequently used in real experiments: (*a*) no constant illumination is applied, bR excited by flashes; (*b*) no flash is applied, equilibrium of the different forms is achieved by constant illumination then the light is swiched off; and (*c*) flashes are applied on the top of constant background illumination.

(*a*) The second term in Eq. 4 is zero and the initial conditions are determined by the intensity of the flashes. The solution is

$$[M_i] = a_i \exp(-t/\tau_i), \qquad (5)$$

and $a_1: a_2: a_3 = f_1: f_2: f_3$ holds for the ratio of the amplitudes. This solution describes the experiments carried out in this study. In the case of vesicles the ratio of the amplitudes is 0.63: 0.35: 0.018 (Table I). Neglecting the third component has only a small effect on the overall M decay curve (see Fig. 1 *b* and *c*). Incorporation of the O form(s) into the model has no effect on this solution, so this type of experiments gives the purest information on the kinetics of the M forms.

(*b*) The second term in Eq. 4 is zero but the initial conditions can be determined from the equilibrium solution of the complete equation. The solution describing the decay after switching the light off is

$$[M_i] = A_i \exp(-t/\tau_i), \qquad (6)$$

where

$$A_i = Cf_i\tau_i$$

and

$$C = 1/(f_1\tau_1 + f_2\tau_2 + f_3\tau_3 + 1/[\sigma\phi]).$$

This results in $A_1: A_2: A_3 = f_1\tau_1: f_2\tau_2: f_3\tau_3$ for the ratio of the amplitudes. For vesicles this ratio is 0.17: 0.56: 0.27. Note that although the time constants are identical with that of the previous case, the amplitudes are extremely different. This causes a completely different overall M decay kinetics which is now very sensitive to neglecting of the third component. The relation between A_i and a_i depends on the model. Incorporation of the O form(s) changes the overall M decay kinetics, so its analysis is more complicated than in the previous case. At the same time, continuous illumination corresponds to the physiological condition. Since the three forms have similar weights in photoequilibrium, any difference in their functions can be important from the physiological point of view. Different ability for proton pumping of two kinetically distinct M forms was recently found by Liu and coworkers (14). This can be one of the

reasons for the inconsistency in the values for the proton stoichiometry published from different laboratories.

(*c*) In this case the second term of Eq. 4 is nonzero, and this makes the analysis of the kinetic data more complicated. Considering only one M form ($f_1 = 1, f_2 = f_3 = 0$), Eq. 4 can be written as

$$[\dot{M}_1] = -[M_1](1/\tau_1 + \sigma\phi) + \sigma\phi, \qquad (7)$$

so the solution will be an exponential with an apparent time constant of $\tau_1/(1 + \tau_1\sigma\phi)$. If more forms exist the relation between the real and the apparent kinetic parameters are more complex. The higher the time constant the higher is the correction needed to get the real parameters. In a previous paper (24) we studied the effect of membrane potential on the kinetics of M decay in cell envelope vesicles. In that work the membrane potential was maintained by continuous background illumination, and the kinetics were studied by applying flashes on the top of it. The data were analyzed in the framework of a model with two parallel M forms. Anomalies were found in the dependence of kinetic parameters on the potential, even when the above corrections were carried out. Taking a third, long lived form into the account, the corrections needed for the time constants as well as the branching probabilities become much higher and can eliminate the anomalies observed. Note that the correction forms are also sensitive to the kinetics of the products of the different forms.

The above analysis shows that apparently negligible long lived forms in the bR photocycle actually can have crucial importance. Introducing new forms into the photocycle the number of the possible models markedly increases. As it was shown, however, the relations among the kinetic parameters depend highly on the experimental conditions as well as on the model used to analyze the data. This means that comparative analysis of experiments carried out under different conditions can select a fewer number of models compatible with the data. Such a systematic study is in progress in our laboratory.

Our experimental data have so far been evaluated by fitting the sum of discrete exponentials to them. With this type of analysis, N exponentials means N individual processes. As an independent approach, one can analyze the data by fitting a (quasi)continuous distribution of exponentials, i.e. determing the $g(k)$ function from Eq. 1. This function can characterize polychromatic reactions (34, 35). Such a reaction takes place if a certain state of a macromolecule consists of numerous conformational substates with slightly different activation energies. In this case one wide peak in $g(k)$ corresponds to essentially one first-order reaction. A polychromatic reaction was found to take place, for example, in CO rebinding in myoglobin (34), in photosystem II luminescence (36) and in the light-induced fast charge displacement in visual rhodopsin (37). It may be expected that the M decay of bacteriorhodopsin can be described better with one distributed rate than with three discrete ones. We applied this type of analysis in an attempt to describe the kinetics of M decay in cell envelope vesicles.

The $g(k)$ functions of M decay in cell envelope vesicles, as calculated by the CONTIN program with three different regularization parameters, are presented in Fig. 7. The magnified residuals of fitting are shown in Fig. 8, and the fitting parameters in Table V. With low regularization the program resulted in a solution with three narrow peaks (Fig. 7 *a*). This picture corresponds to three different

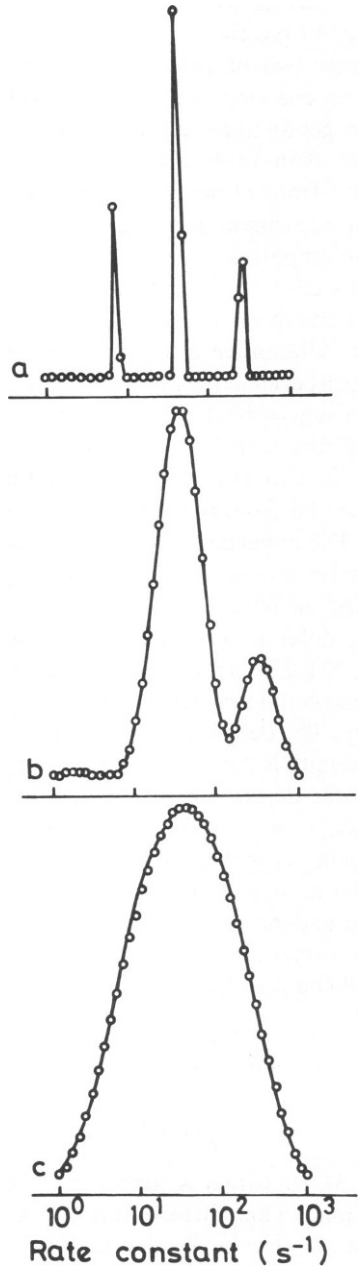

FIGURE 7 The $g(k)$ function of Eq. 1 fitted to the decay of the M form(s) in cell envelope vesicles. For experimental conditions see legend of Fig. 1. Calculation was performed with three different regularization parameters (α) (*a*) $\alpha = 8.80 \times 10^{-7}$; (*b*) $\alpha = 1.09 \times 10^{-2}$; and (*c*) $\alpha = 1.21$. See Table V for the fitting parameters.

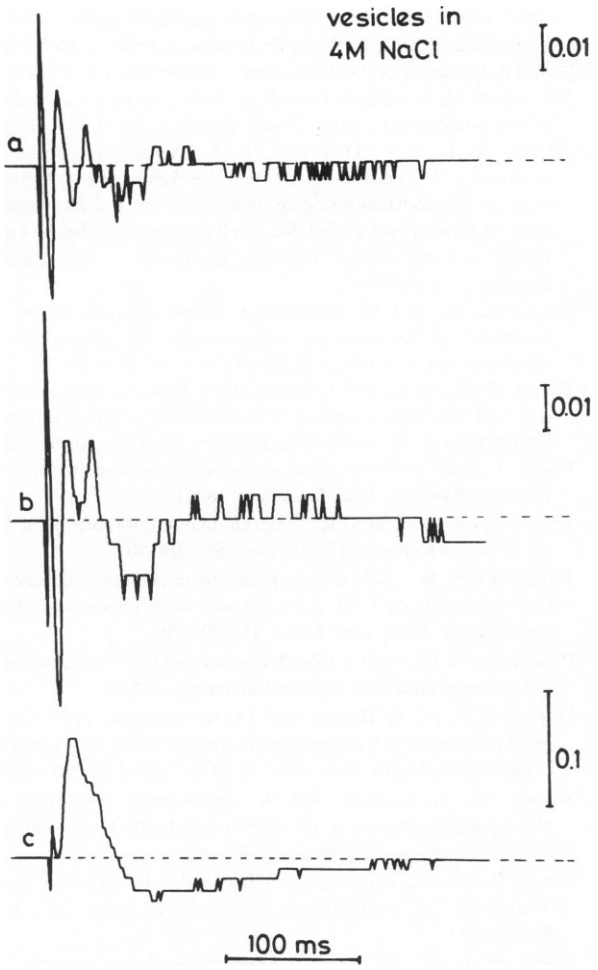

FIGURE 8 Magnified residuals corresponding to the fitting with $g(k)$ functions (*a*), (*b*), and (*c*), respectively in Fig. 7. The residuals were normalized as in Fig. 2. See Table V for the fitting parameters.

individual first-order processes. The positions of the peaks and the areas under them correlate well with the time constants and amplitudes calculated by the fitting of three discrete exponentials (see Table I). The standard deviation of this solution is higher than that of the three discrete exponentials. This is probably due to the small number of points in g_k.

With increased regularization we obtained a solution consisting of two wider peaks (Fig. 7 *b*). This corresponds to two different polychromatic reactions. Interestingly, the residuals and the standard deviations of this solution are hardly higher than that of the solution with three peaks. Considering the ill-posed nature of this type of calculation (see Materials and Methods), neither of these functions can be preferred on the basis of the statistical parameters.

The third solution of $g(k)$ is a single, very wide peak (Fig. 7 *c*). This would correspond to a single polychromatic reaction. However, since the residuals and the standard deviations are very high, this solution has to be rejected.

In summary, we suggest that on the basis of the above two types of calculation the kinetics of the *M* decay of bacteriorhodopsin at high ionic strength can be characterized either by three individual first-order processes (probably corresponding to three parallel *M* forms) or by two polychromatic reactions.

TABLE V
PARAMETERS OF CONTINUOUS DISTRIBUTION FUNCTIONS OF EXPONENTIALS FITTED TO THE DECAY OF THE *M* FORMS IN CELL ENVELOPE VESICLES

α	8.80×10^{-7}	1.09×10^{-2}	1.21
A_1*	0.03	—	—
τ_1‡	143	—	—
A_2	0.33	0.33	1
τ_2	24.3	28.9	28.9
A_3	0.64	0.67	—
τ_3	3.46	2.89	—
S§	5.16	8.23	27.93

*The sum of the areas under the peaks is normalized to 1.
‡In milliseconds.
§S = (standard deviation)/(maximum of signal) $\times 10^3$.
(A_i = areas under the peaks, $\tau_i = 1/$(position of the maximum of peaks). Calculations were performed with different regularization parameters (α).

Thanks are due to Drs. J. Czege, B. Szalontai, and L. Viragh for their help with the experiments, and Drs. Cs. Bagyinka and J. Posfai for help with the computer program. Prof. L. Keszthelyi called our attention to the polychromatic reactions. Dr. J. Gargyan, Mrs. E. Hegedus, and Mr. M. Szucs provided excellent technical assistance.

Received for publication 17 September 1985 and in final form 27 February 1986.

REFERENCES

1. Lozier, R. H., R. A. Bogomolni, and W. Stoeckenius. 1975. Bacteriorhodopsin: a light-driven proton pump in *Halobacterium halobium*. *Biophys. J.* 15:955–962.
2. Slifkin, M. A., and S. R. Caplan. 1975. Modulation excitation spectrophotometry of purple membrane of *Halobacterium halobium*. *Nature (Lond.)*. 253:56–58.
3. Lozier, R. H., W. Niedeberger, R. H. Bogomolni, S. B. Hwang, and W. Stoeckenius. 1976. Kinetics and stoichiometry of light-induced proton release and uptake from purple membrane fragments, *Halobacterium halobium* cell envelopes, and phospholipid vesicles containing oriented purple membrane. *Biochim. Biophys. Acta.* 440:545–565.
4. Korenstein, R., and B. Hess. 1977. Hydration effects on the photocycle of bacteriorhodopsin in thin layers of purple membrane. *Nature (Lond.)*. 270:184–186.
5. Lozier, R. H., and W. Niederberger. 1977. The photochemical cycle of bacteriorhodopsin. *Fed. Proc.* 36:1805–1809.
6. Korenstein, R., B. Hess, and D. Kuschmitz. 1978. Branching reactions in the photocycle of bacteriorhodopsin. *FEBS (Fed. Eur. Biochem. Soc.) Lett.* 93:266–270.
7. Korenstein, R., B. Hess, and M. Marcus. 1979. Cooperativity in the photocycle of purple membrane *Halobacterium halobium* with a mechanism of free energy transduction. *FEBS (Fed. Eur. Biochem. Soc.) Lett.* 102:155–161.
8. Kriebel, A. N., T. Gillbro, and U. P. Wild. 1979. A low temperature investigation of the intermediates of the photocyle of light-adapted bacteriorhodopsin. Optical absorption and fluorescence measurements. *Biochim. Biophys. Acta.* 546:106–120.

9. Nagle, J. F., L. A. Parodi, and R. F. Lozier. 1982. Procedure for testing kinetic models of the photocycle of bacteriorhodopsin. *Biophys. J.* 38:161–174.
10. Eisenbach, M., E. P. Bakker, R. Korenstein, and S. R. Caplan. 1976. Bacteriorhodopsin biphasic kinetics of phototransients and of light-induced proton transfer by sub-bacterial *Halobacterium halobium* particles and by reconstituted liposomes. *FEBS (Fed. Eur. Biochem. Soc.) Lett.* 71:228–232.
11. Ort, D. R., and W. W. Parson. 1978. Flash induced volume changes of bacteriorhodopsin containing membrane fragments and their relationship to proton movements and absorbance transients. *J. Biol. Chem.* 253:6158–6164.
12. Govindjee, R., T. G. Ebrey, and A. R. Crofts. 1980. The quantum efficiency of proton pumping by the purple membrane of *Halobacterium halobium. Biophys. J.* 30:231–242.
13. Kuschmitz, D., and B. Hess. 1981. On the ratio of the proton pump and photochemical cycles in bacteriorhodopsin. *Biochemistry.* 20:5950–5957.
14. Li, Q. -Q., R. Govindjee, and T. G. Ebrey. 1984. A correlation between proton pumping and the bacteriorhodopsin photocycle. *Proc. Natl. Acad. Sci. USA.* 81:7079–7082.
15. Gilbro, T. 1978. Flash kinetic study of the last steps in the photoinduced reaction cycle of bacteriorhodopsin. *Biochim. Biophys. Acta.* 504:175–186.
16. Edgerton, M. E., and C. Greenwood. 1979. Evidence for a model of regeneration of protonated species, bR, from a phototransient, M, in the photochemical cycle of bacteriorhodopsin from *Halobacterium halobium. Biochem. Soc. Trans.* 7:1075–1077.
17. Ohno, K., Y. Takeuchi, and M. Yoshida. 1981. On the two forms of intermediate M of bacteriorhodopsin. *Photochem. Photobiol.* 33:573–578.
18. Lam, E., and L. Packer. 1983. Nonionic detergent effects on spectroscopic characteristics and the photocycle of bacteriorhodopsin in purple membrane. *Arch. Biochem. Biophys.* 221:557–564.
19. Mathew, K. A., S. L. Helgerson, D. Bivin, and W. Stoeckenius. 1985. Two kinetically and spectrally distinct M intermediates in the photocycle of bacteriorhodopsin. *Biophys. J.* 47 (2, Pt. 2):323*a* (Abstr.)
20. Deng, H., C. Pande, R. H. Callender, and T. G. Ebrey. 1985. A detailed resonance Raman study of the M_{412} intermediate in the bacteriorhodopsin photocycle. *Photochem. Photobiol.* 41:467–470.
21. Parodi, L. A., R. H. Lozier, S. M. Bhattacharjee, and J. F. Nagle. 1984. Testing kinetic models for the bacteriorhodopsin photocycle—II. Inclusion of an O to M backreaction. *Photochem. Photobiol.* 40:501–512.
22. Dancshazy, Zs., S. L. Helgerson, and W. Stoeckenius. 1983. Coupling between the bacteriorhodopsin photocycle kinetics and the protonmotive force. I. Single flash measurements in *Halobacterium halobium* cells. *Photobiochem. Photobiophys.* 5:347–357.
23. Westerhoff, H. V., and Zs. Dancshazy. 1984. Keeping a light-driven proton pump under control. *Trends Biochem. Sci.* 9:112–116.
24. Groma, G. I., S. L. Helgerson, P. K. Wolber, D. Beece, Zs. Dancshazy, L. Keszthelyi, and W. Stoeckenius. 1984. Coupling between the bacteriorhodopsin photocycle and the protonmotive force in *Halobacterium halobium* cell envelope vesicles. II. Quantitation and preliminary modeling of the M → bR reactions. *Biophys. J.* 45:985–992.
25. Oesterhelt, D., and W. Stoeckenius. 1974. Isolation of the cell membrane of *Halobacterium halobium* and its fractionation into red and purple membrane. *Methods Enzymol.* 31:667–678.
26. Der, A., P. Hargittai, and J. Simon. 1985. Time-resolved photoelectric and absorption signals from oriented purple membranes immobilized in gel. *J. Biochem. Biophys. Methods.* 10:295–300.
27. Czege, J. 1983. Intelligent flash photolysis measuring system. *Acta Biochim. Biophys. Acad. Sci. Hung.* 18:90.
28. Bagyinka, Cs. 1982. SPSERV program manual. Reports of Biological Research Center of Hung. Acad. Sci., BF-001.
29. Provencher, S. W. 1979. Inverse problems in polymer characterization: Direct analysis of polydispersity with photon correlation spectroscopy. *Makromol. Chem.* 180:201-209.
30. Provencher, S. W. 1980. CONTIN Users manual. Technical report of European Molecular Biology Laboratory, DA02.
31. Hanamoto, J. H., P. Dupuis, and M. A. El-Sayed. 1984. On the protein (tyrosine)-chromophore (protonated Schiff base) coupling in bacteriorhodopsin. *Proc. Natl. Acad. Sci. USA.* 81:7083–7087.
32. Kimura, Y., A. Ikegami, and W. Stoeckenius. 1984. Salt and pH-dependent changes of the purple membrane absorption spectrum. *Photochem. Photobiol.* 40:641–646.
33. Chang, C.-H., J.-G. Chen, R. Govindjee, and T. Ebrey. 1985. Cation binding by bacteriorhodopsin. *Proc. Natl. Acad. Sci. USA.* 82:396–400.
34. Austin, R. H., K. W. Beeson, L. Eisenstein, H. Frauenfelder, and I. C. Gunsalus. 1975. Dynamics of ligand binding to myoglobin. *Biochemistry.* 14:5355–5373.
35. Goldanskii, V. I. 1979. Facts and hypotheses of molecular chemical tunnelling. *Nature (Lond.).* 279:109–115.
36. Lavorel, J., and J.-M. Dennery. 1982. The slow component of photosystem II luminescence. A process with distributed rate constant? *Biochim. Biophys. Acta.* 680:281–289.
37. Lindau, M., and H. Ruppel. 1983. Evidence for conformational substates of rhodopsin from kinetics of light-induced charge displacement. *Photobiochem. Photobiophys.* 5:219–228.